

Bubble Bursting and Stall Hysteresis on Single-Slotted Flap High-Lift Configuration

M. Baragona,* L. M. M. Boermans,† M. J. L. van Tooren,‡ H. Bijl,§ and A. Beukers‡
Delft University of Technology, 2629 HS Delft, The Netherlands

Slotted multi-element configurations are widely used because they are very effective in increasing the maximum lift of airfoils during takeoff and landing. However, when stall occurs in the leading-edge region of one of the elements, the outcome is a sudden and dangerous drop in performance of the whole configuration. The results of the experimental verification of a computer-designed single-slotted flap are presented. Many realistic configurations, including the computed optimum, were tested and compared to the numerical predictions. For a number of these configurations, sudden leading-edge stall due to the bursting of a laminar bubble was detected on the flap, followed by severe stall hysteresis. Present numerical design codes do not help the designer much in predicting this important phenomenon, and wind-tunnel testing remains necessary. Therefore, there is a need for better bubble bursting prediction methods. A possible direction for improvement is discussed, focusing on the unsteadiness of the flow.

Nomenclature

C_d	=	drag coefficient
C_l	=	lift coefficient
$C_{l_{max}}$	=	maximum lift coefficient
C_p	=	pressure coefficient
c	=	aerodynamic chord with flap nested
R_k	=	refinement ratio
Tu	=	freestream turbulence level, $\sqrt{u'^2}/V$
U	=	uncertainty
V	=	velocity
x, y	=	coordinates
α	=	angle of attack
δ	=	displacement thickness
θ	=	momentum thickness

Introduction

THE main focus of high-lift design is to maximize the $C_{l_{max}}$, whereas less attention is devoted to poststall flow development. This practice can lead to a dangerous optimum design, especially for Reynolds numbers up to an order of 10^6 when laminar separation bubbles are involved. The bursting of a laminar bubble causes a hysteresis loop in the curve $C_l-\alpha$ that can turn out to be rather large. The result is a very dangerous situation because of the combination of the sudden lift loss and the large $\Delta\alpha$ reduction that is needed to resume prestall conditions. This is particularly relevant for the flap of a multi-element configuration where the possible occurrence of such a situation has only recently been discovered.

The formation of laminar bubbles on the leading edge of a single-element airfoil and their possible bursting are known to affect strongly the stall behavior of single-element airfoils. The possibility of bursting and stall hysteresis, however, is often disregarded during the design process. When experiments are done, it is not uncommon that tests are stopped just after stall occurs, with no interest

in poststall behavior. On the other hand, existing bubble bursting predictors perform badly, especially in the low-Reynolds-number Re range, unless an accurate and dedicated tuning against available (if any) experiments is performed.¹ The most widespread numerical design codes for single and multi-element airfoils, for example, XFOIL,² MSES³ and the Eppler code,⁴ lack the required accuracy to predict stall behavior and do not include any of these bursting predictors. The designer currently relies heavily on experimental analysis, much more than for cruise conditions.

In this paper, the two-dimensional physics and airfoil design issues in relation to bubble bursting, will be addressed. The two-dimensional case permits a much deeper and detailed investigation of the driving flow phenomena⁵ than does the three-dimensional approach and for ordinary unswept wings, three-dimensional effects are usually limited to a small region near the tip. (A definition of the global characteristics of three-dimensional separation and of its topology is still a matter of discussion.^{6,7}) In addition, transition at low Reynolds numbers develops mainly as a two-dimensional process. All evidence suggests that the amplification of three-dimensional disturbances by secondary instabilities is in fact less rapid in this case, being somehow "locked" on a dominant two-dimensional wave frequency.⁸

First, a review of the present theoretical knowledge on laminar bubbles will be given. Also, a parallel will be drawn between the multi-element and the single-element case. In the following sections, the experimental and numerical results obtained during and after the design process of a multi-element single-slotted flap configuration will be presented. Finally, a number of physical aspects will be addressed that are not included in the classical model of a laminar bubble and, hence, not accounted for in the existing bursting prediction methods, indicating a possible direction for improvement.

The experimental and numerical results show that the bubble present in the nose region of the flap of this slotted configuration was extremely important in determining the performance of the whole multi-element configuration. When this bubble burst and the flap stalled, a sudden loss of lift and a large hysteresis loop followed, a behavior similar to that observed in the single-element case. This is an important and rather new finding^{9,10} because the possibility of bursting and stall hysteresis is usually ignored in the process of designing a new flap. The Reynolds number range where this bursting may happen is found to be higher than for single-element airfoils. The experiments shown in this paper were carried out at a Reynolds number of about 2×10^6 , as required by the specifications of the Eaglet two-seater training motor plane for which the flap had been designed. This value of 2×10^6 is a typical value for general aviation airplanes in landing conditions. Hence, it may be expected that the findings for the current setup should have a more general significance and that the possibility of bursting should be regarded as a

Received 22 March 2002; revision received 3 February 2003; accepted for publication 4 February 2003. Copyright © 2003 by the authors. Published by the American Institute of Aeronautics and Astronautics, Inc., with permission. Copies of this paper may be made for personal or internal use, on condition that the copier pay the \$10.00 per-copy fee to the Copyright Clearance Center, Inc., 222 Rosewood Drive, Danvers, MA 01923; include the code 0001-1452/03 \$10.00 in correspondence with the CCC.

*Research Fellow, Department of Aerospace Engineering, Kluuyverweg 1.
†Associate Professor, Department of Aerospace Engineering, Kluuyverweg 1.

‡Professor, Department of Aerospace Engineering, Kluuyverweg 1.

§Assistant Professor, Department of Aerospace Engineering, Kluuyverweg 1.

major danger during the design of a flap for low-Reynolds-number applications.

Theoretical Background

A laminar boundary layer may reach the separation point before transition to a turbulent layer is achieved. For each airfoil shape and thickness, this will happen at a certain combination of Reynolds number, freestream turbulence level Tu , and angle of attack α . For any airfoil at a relatively low turbulence level and a given α , there exists a value of the Reynolds number below which laminar separation occurs. The flow development after the separation point depends strongly on the behavior of the separated laminar shear layer. It is thought that, due to its high instability, transition to turbulence occurs shortly after the separation point, increasing the entrainment with the external flow, and, thus, causing reattachment to the surface and the formation of a region of relatively stagnant flow, a short bubble (Fig. 1). However, at high angles of attack or at low Reynolds numbers, the flow may become unable to overcome the adverse pressure gradient and fail to reattach. The flow pattern will then change into a so-called long bubble or into a completely separated flow (leading-edge stall).

In this view, bubble bursting can, therefore, be seen as either the momentary breakdown (in case of long bubble formation) or definitive breakdown (in case of leading-edge stall) of the turbulent shear layer reattachment process. No physical difference exists between the long and the short bubble in this model. The difference lies only in the effect of the bubble on the pressure distribution: local and limited in the case of a short bubble, more influential in the case of a long bubble.

Stall Hysteresis on a Single-Element Airfoil

Once bubble bursting occurs, a hysteresis loop in the C_l - α curve is observed. When it is present, this loop represents a real danger for pilots. The main reason why uncovering the physics behind the bursting of a laminar bubble is such an important issue is to be able to prevent stall hysteresis occurrence.

A review of hysteresis can be found in Ref. 9 both for fixed and rotary wings. Here the concern is particularly with fixed-wing aircraft, where the phenomenon is usually referred to as stall hysteresis. A short description of a typical hysteresis loop may be given as follows. By raising α , the laminar bubble first moves toward the leading edge, diminishing its length. Suddenly it bursts, turning into a completely separated flow or into a long bubble, which widens toward the trailing edge of the profile until, ultimately, the flow is completely separated. If at this stage α is decreased, the flow will remain separated for a while before the bubble is reformed, thus, giving rise to the observed loop in the C_l - α curve. Notice that at low Reynolds number Re almost every airfoil experiences this kind of hysteresis loop, even if sometimes at such a high α value that it is not captured during usual experimental tests. Also, as shown by Gault,¹¹ bubble bursting can happen also at high Reynolds numbers if the curvature of the nose is high enough. In many cases, including the NASA experiments on which Gault's work was based,

the hysteresis is not detected because in the experiments the angle of attack was not reduced after bubble bursting.

Slotted Multi-Element Configuration

The idea to split an airfoil in more elements dates back to the end of the first World War when a German engineer-pilot, G. V. Lachmann (who had just survived a crash following a stall during its early training flights), first proposed it to Prandtl. The results of the ensuing experimental tests were indeed encouraging, in some cases with spectacular lift increase beyond 30% of the basic value, demonstrating the validity of the proposal. However, the principle on which it works has been misinterpreted for many years after these early applications. It has become clearer that the slot does not work as a boundary-layer control device, but, as Smith¹² pointed out, owes its remarkable performance mainly to the change it produces in the characteristics of the external inviscid flow. The pressure rise over the whole configuration is split into a number of less severe pressure rises, thus, leading to the large overall lift increase observed in the experiments. Both the circulation around the main airfoil and the effect of its wake act in the direction of reducing the pressure peak in the nose region of the flap, which can then delay separation and in turn raise the circulation and the lift contribution of the main element. Another important feature is that each element has a new boundary-layer development. However, when large separated regions, usually on the flap surface, are present, viscous effects become decisive and they place an upper limit to the achievable lift increase.

Stall Hysteresis on a Slotted Multi-Element Configuration

Although it is a well known and identified flow feature in the case of single-element airfoils, the possibility of stall hysteresis over multi-element configurations seems to be poorly known, and there is little in the literature about the subject.

Like for the single-element case, bubble bursting and stall hysteresis are readily connected. The flow on the flap behaves in a very similar way, displaying after bursting a typical leading-edge stall pattern. In the slotted multi-element case, the main element wake and the direction and the strength of the slot flow are very important additional factors that are absent in the single-element case. They strongly affect the flow development on the flap and the eventual burst of the bubble in its nose region. Because of the reduced pressure gradient, the boundary layer over the flap tends to stay laminar longer, provided that turbulence contamination from the main airfoil wake is avoided. In addition, the chord of the flap is much shorter than the main airfoil, so that a scale effect on the Reynolds number Re is present. In our case, an upstream $Re = 2 \times 10^6$ becomes a $Re = 4.36 \times 10^5$ when based on the 21.8% chord of the flap, clearly falling in the range where stall hysteresis is more likely to occur on single-element airfoils. This effect is much stronger once the gap (Fig. 2) is made wider because the flow around the flap

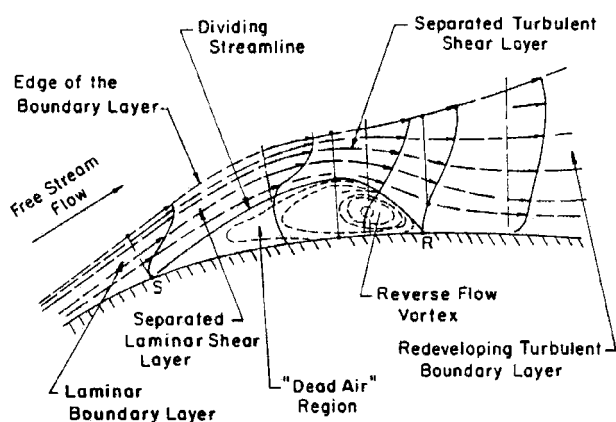


Fig. 1 Classical structure of a short laminar bubble.¹⁶

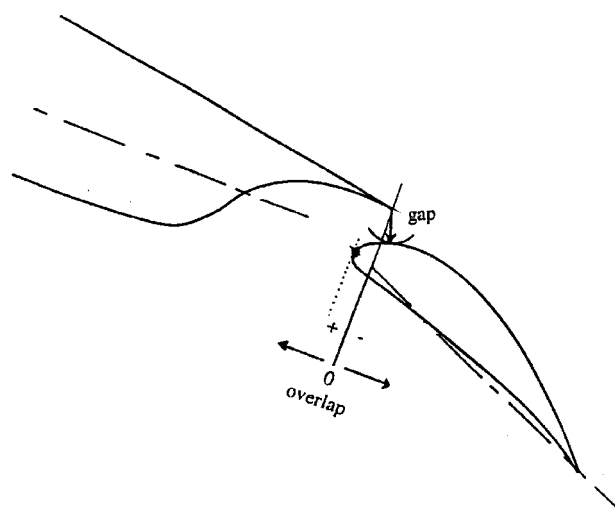


Fig. 2 Gap and overlap definition.

becomes less dependent on the flow over the main element. When bubble bursting occurs on the flap, the pressure distribution over the flap surface suddenly collapses. The reduced circulation of the flap in turn reduces the circulation of the main element, leading to a global effect on the flow over the entire airfoil system. Here again, the angle of attack must be lowered considerably before the flap again reaches prestall conditions, giving rise to the observed hysteresis loop. Hence, the bursting on the flap controls the hysteresis on a multi-element airfoil.

Difficulties in Current High-Lift Design Practice

Numerical Modeling Difficulties

Both stall and poststall behavior should be taken into account to achieve an optimum high-lift design. For a prediction of poststall evolution, a Navier–Stokes code or at least a dedicated treatment of the separated region would be required.¹³ The use of a Navier–Stokes code, however, is usually not an option for high-lift design purposes. There are two main reasons for this. The first one is more general and also is valid when laminar bubbles are absent, that is, the large computational time involved and the high number of parameter combinations that should be tested. The second is that the physics of bursting and the mechanism of transition, especially close to or after bursting, are not clear yet and, thus, no reliable model is available. An unsteady direct numerical simulation solver would then be required. This option is currently not viable, not only for design purposes.

As a numerical tool for two-dimensional high-lift design, boundary-layer codes are at present the usual choice, for both single-element airfoils and for multi-element high-lift configurations. Although some of these codes can deal even with large separated regions, the results are not as satisfactory as for attached flows,¹⁴ ultimately leading to the breakdown of the code when the separated region becomes too extensive. Hence, for the problem analyzed here, not more than a warning on bubble bursting occurrence can be expected. An accurate prediction of the onset of bursting is very important because parameter changes leading to $C_{l_{\max}}$ improvement are also driving bubble bursting occurrence and because of the strong link between bursting and the hysteresis phenomenon.

Many semi-empirical methods to predict bursting onset have been proposed in the past (for instance, Crabtree,¹⁵ Horton,¹⁶ van Ingen,¹⁷ Dini and Maughmer,¹⁸ and Shum¹). None of them, however, successfully predict bubble bursting in all flow conditions, especially in the low-Reynolds-number Re range, where they require a very accurate tuning to work well. This tuning is time consuming and extremely difficult when no previous experimental data are available. For this reason, these methods are not practical, and most boundary-layer codes for design purposes do not include them. In addition, these codes usually show no sign of breakdown when close to the conditions when bursting occurs in the experiments. As a result of these modeling difficulties, experimental tests are necessary to verify the numerical design.

Flap of the Eaglet

In the present investigation, one of the most widespread and efficient boundary-layer design codes, the MSES code developed by Drela,³ was used for the design of a single slotted flap for the Euro-ENAER Eaglet utility aircraft⁹ starting from a NACA 63-415 airfoil section. The optimum geometry was checked in the Low Speed Wind Tunnel (LTT) of the Delft University of Technology.²⁰ The analysis for the cruise configuration was found satisfactory, but when testing the landing configuration (30-deg flap deflection and $Re = 2 \times 10^6$), large discrepancies with the numerical predictions were found. In the next sections, first the experimental results will be shown and then the numerical calculations.

Experimental Investigation

Experimental Setup

The LTT of the Delft University of Technology is a closed-return-type wind tunnel with a contraction ratio of 17.9 (Ref. 20). The test section is 1.8 m wide, 1.25 m high, and 2.6 m long. The tunnel is

designed for a maximum speed in the test section of 120 m/s. The turbulence level varies from 0.018% at 10 m/s up to 0.1% at 100 m/s. To prevent separation at wing–wall junctions, suction boxes were attached to the test section wall during this investigation. The amount of suction was chosen according to Foster and Lawford,²¹ and the resulting flow behavior was checked through tufts applied near the trailing edge of the flap and main element surfaces.

The composite wind-tunnel model has a flap nested chord of 0.6 m and a span of 1.25 m. The flap chord is 21.8% of the flap nested chord. The model was installed vertically in the test section and equipped with a total of 59 pressure orifices on the main wing and 23 on the flap (0.4-mm diam) located in diagonal rows between 0.45 and 0.55 m from the top of the test section. The surface of the model consists of polyester gelcoat, which has been polished to ensure an aerodynamically smooth finish.

A total and static pressure wake rake, mounted on a cross beam, was positioned behind the model, with the tips of the total pressure tubes at 57% of the chord c downstream of the flap trailing edge. A pitot static tube was mounted on the side wall in front of the model, at about two chord lengths from the leading edge. All pressure taps were connected to a multitube liquid manometer (200 tubes) equipped with an automatic infrared reading device. The measured pressure coefficients were numerically integrated (trapezium rule) to obtain the main element and flap normal force and pitching moment coefficients. The section profile drag coefficient was computed from the wake rake total and static pressures using the Jones method.²² Standard low-speed wind-tunnel boundary corrections have been applied to the data according to the method of Allen and Vincenti.²³

Experimental Accuracy

The automatic reading device reads the manometer tubes with an accuracy of 0.1 mm, that is, 1 Pa. Because of the need of a reference run, the accuracy in the measured pressure values is 2 Pa. A specially developed speed control system is installed in the wind tunnel, accurate within 0.02% of the set speed. When these values are taken into account, the uncertainty U_{C_p} of the measured C_p can be estimated.²⁴ Focusing on the 3.0% gap/1.0% overlap arrangement, we estimate a value of $U_{C_p} = \pm 0.00179513$ at 0 deg and a value of $U_{C_p} = \pm 0.00430969$ at 10 deg. These are roughly the largest and smallest uncertainties for the 3.0% gap/1.0% overlap arrangement. The uncertainties are the same order of magnitude for the other arrangements as well. The uncertainty U_α in the angle of attack is $U_\alpha = \pm 0.01$ deg. The uncertainty in the gap and overlap measurements, $U_{g,o}$, is estimated to be about 0.1 mm, hence, 0.02% of the chord ($U_{g,o} = \pm 0.02\%$). The uncertainty in the integrated quantities is more difficult to estimate. It depends on the spacing between the orifices, and it is higher in the regions of high-pressure gradients, that is, close to the nose. Errors due to three dimensionality of the flow were minimized by the suction applied at the wing–wall junctions.

Experimental Results

All pressure distributions presented in this section are measured with a gap of 3% and an overlap of 1% of the chord c . However, lift and drag curves from other flap settings are also presented to show the trends resulting from changes in gap–overlap. All results shown are relative to the flap in landing configuration (30-deg deflection). A scheme relating the gap–overlap settings to the occurrence of the hysteresis loop is shown in Fig. 3. The effect of a change in gap dimension was particularly investigated. For the overlap, only two different setups were checked, 1 and 2%. As can be seen in Fig. 3, a rise in the gap increases the possibility of a hysteresis loop. For a gap value of 1.5%, no hysteresis was observed. On the other hand, for a gap value of 4%, the flow over the flap was always separated at all measured angles of attack. Changes in the overlap value around the computed optimum position seemed to be less relevant to the occurrence of hysteresis than a change in the gap. However, for 2.0% gap, hysteresis was observed for an overlap value of 1%, but not for an overlap of 2%. For a 1% overlap and 2.5 and 3.0% gap values, the flap was separated at the beginning of the measurements ($\alpha = 0$), and α had to be lowered first, before obtaining an attached

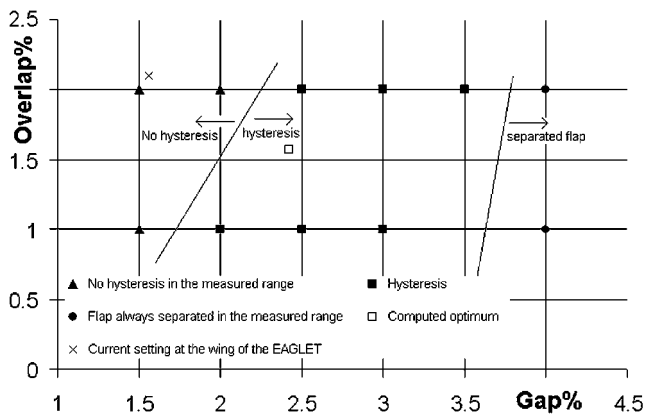
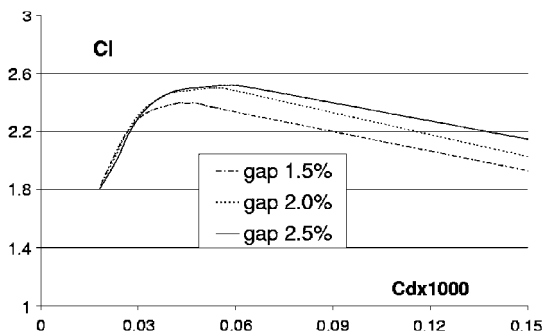
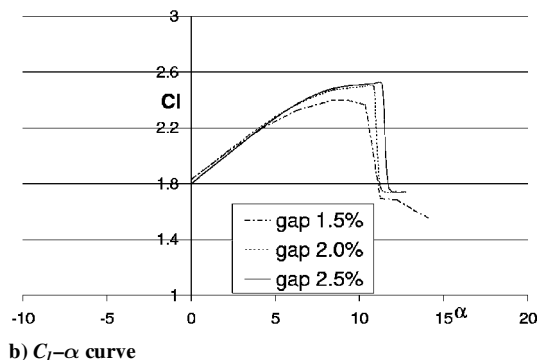


Fig. 3 Observed relationship between gap-overlap and hysteresis occurrence in the measured range from $\alpha \sim -6$ to $\alpha \sim 16$ deg, $Re = 2 \times 10^6$, NACA 63-415 airfoil with slotted flap.



a) C_l-C_d curve



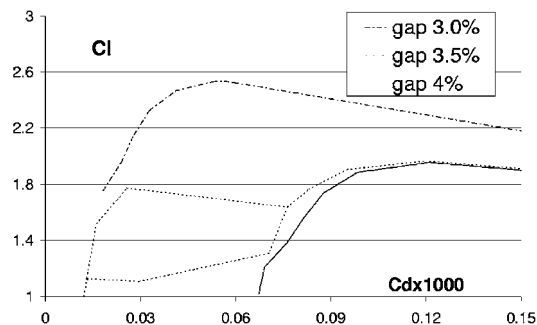
b) $C_l-\alpha$ curve

Fig. 4 Effect of gap variation before bursting occurrence (overlap 2.0%), $Re = 2 \times 10^6$, NACA 63-415 airfoil with slotted flap.

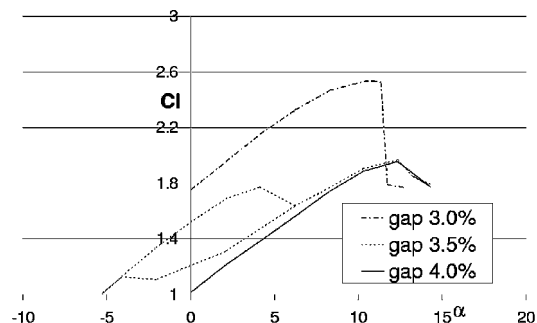
flow on the flap surface. This effect is rather peculiar and is reported also by Biber.⁹

When bubble bursting does not occur, a wider gap enhances the performance of the configuration in terms of lift coefficient. This effect can be seen clearly in Fig. 4, where the C_l-C_d polar and the lift curve for 1.5, 2.0, and 2.5% gap, with 2.0% overlap, are shown. The maximum C_l increases by increasing the gap, ranging from $C_{l_{max}} = 2.4$ to $C_{l_{max}} = 2.5$ upto $C_{l_{max}} = 2.52$, respectively. However, a wider gap also increases the danger of bubble bursting over the flap surface, as can be seen in Fig. 5, where the C_l-C_d polar and the lift curve for 3.0, 3.5, and 4% gap, with 2.0% overlap, are shown. The maximum C_l drops from a value of $C_{l_{max}} = 2.53$ for gap 3.0% to $C_{l_{max}} = 1.9$ for 3.5 and 4% gaps. This represents a quite critical issue when designing a flap because it is easy to make the gap too wide if bubble bursting is not taken into account properly. The hysteresis loop for gap 3.5% is also shown in Fig. 5.

The 3% gap and 1% overlap case was chosen for detailed investigation of stall hysteresis and comparison with the numerical analysis. The large clockwise hysteresis loop that occurred in this case can be clearly seen from the C_l-C_d and $C_l-\alpha$ curves shown in Fig. 6. (The numerical results will be discussed in the next sections.)

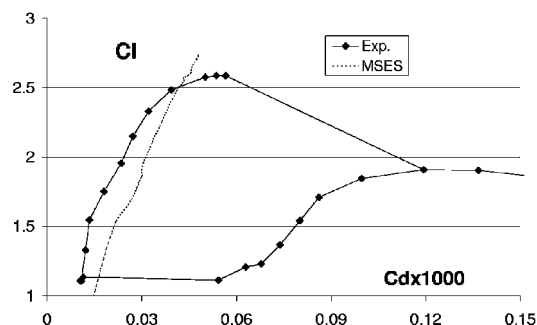


a) C_l-C_d curve

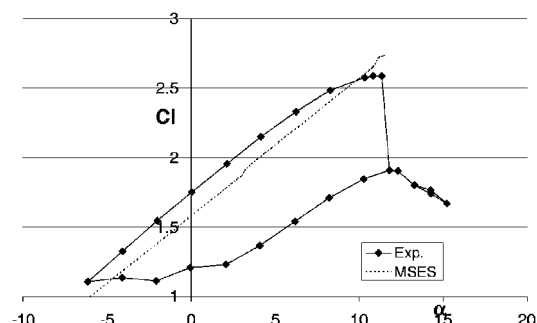


b) $C_l-\alpha$ curve

Fig. 5 Experimental drag and lift coefficient for gap 3.5, 4, and 3.0% (overlap 2.0%) showing the hysteresis loop for the 3.5% case, $Re = 2 \times 10^6$, NACA 63-415 airfoil with slotted flap.



a) C_l-C_d curve



b) $C_l-\alpha$ curve

Fig. 6 Gap 3% overlap 1%: experimental results and computational predictions (see also Fig. 7), $Re = 2 \times 10^6$, NACA 63-415 airfoil with slotted flap.

The corresponding pressure distributions are shown in Fig. 7 for some representative angles of attack covering the entire hysteresis loop. At the beginning of this test ($\alpha = 0$), right after turning on the wind tunnel, the flow over the flap was completely separated. The flow attached only after α had been lowered to -6 deg (Fig. 7a). From this starting value, the pressure distributions on the flap and main airfoil were recorded. Raising α from -6 up to 11 deg (Figs. 7a-7f), the flow on the flap stayed attached. The main airfoil

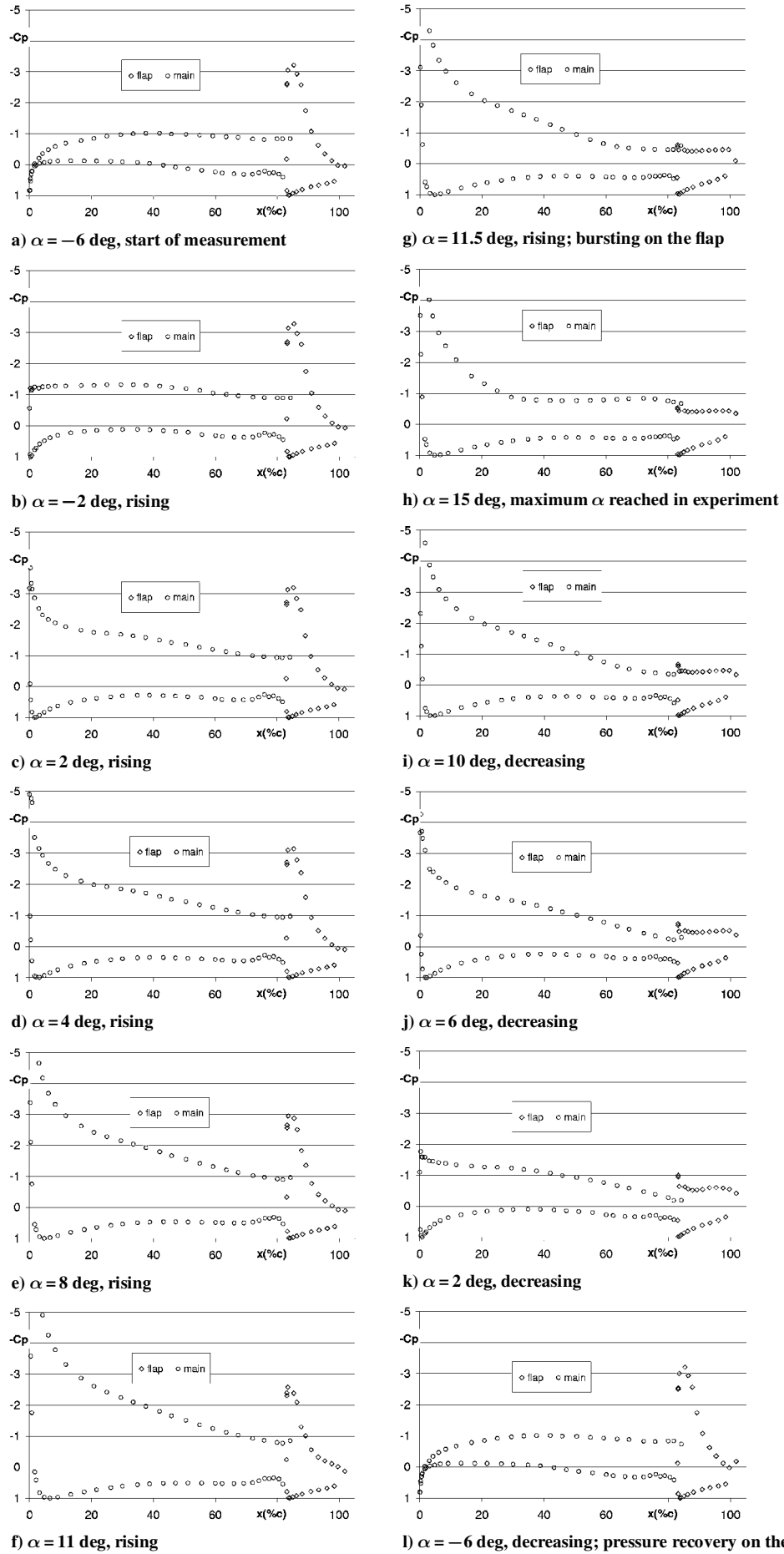


Fig. 7 Hysteresis loop for gap 3% overlap 1%: pressure distribution, $Re = 2 \times 10^6$, NACA 63-415 airfoil with slotted flap.

kept on gaining lift, while the pressure peak on the flap nose was slightly reduced as α was increased. From Fig. 6b it can be seen that the C_l of whole configuration increased up to a maximum of about $C_{l_{\max}} = 2.6$ for $\alpha = 11$ deg. At $\alpha = 11.5$, however, the pressure distribution over the flap suddenly leveled, as can be seen in Fig. 7g. As a result, the C_l dropped to a value of about $C_{l_{\max}} = 1.9$ (Fig. 6b) while the C_d increased to almost twice its value before bursting (Fig. 6a). The angle of attack was still raised up to 15 deg (Fig. 7h). The trailing-edge separation on the main element, which could hardly be noticed in Figs. 7f and 7g, is now covering most of the main element surface, resulting in further C_l loss and C_d increase (Fig. 6). When the angle of attack was lowered, the flow on the flap stayed separated far beyond the value of $\alpha = 11.5$ deg where bursting first occurred (Figs. 7i–7k), causing the hysteresis loop of Fig. 6b. The angle of attack had to be lowered to -6 deg to obtain again an attached flow on the flap (Fig. 7l).

In this case, the reason for the hysteresis occurrence is readily identified with the flap flow behavior. The pressure distributions show that the flow over the flap separated suddenly with the characteristics of a leading-edge-type stall due to bubble bursting. Meanwhile, no major trailing-edge separation on the main wing was detected at this bursting onset (Figs. 7f and 7g). Such trailing-edge separation on the main airfoil has been reported on other multi-element configurations⁹ and appears after bursting also in the present analysis, as can be seen from the pressure distribution at 15 deg. However, at bursting (for α between 11 and 11.5 deg), while the pressure over the flap is leveled, only the effect due to the loss of circulation is evident on the main wing. The flow appears to be separated close to the trailing edge of the main element but in this case this seems to be the consequence rather than the cause of the separation on the flap.

Computational Investigation

The MSES code solves the Euler equations strongly coupled to a two-equations integral boundary-layer formulation. Two-point central differencing is generally used to discretize the boundary-layer equations. A transition prediction method of the e^n type²⁵ is included in the viscous formulation. The complete set of equations is then solved by a global Newton method so that strong viscous-inviscid interactions can be taken into account.³ MSES has proven to be a very useful tool for multicomponent airfoil design purposes. It is currently widely used for the design of many successful airfoils. Large separation regions can, in principle, be handled, although, as for all other boundary-layer codes,¹⁴ the results are less accurate. The code is a steady solver, and thus, no unsteady effects can be captured. As for all other codes for design purposes, MSES does not include any bursting criterion, and no warning regarding its possible onset is given to the designer.

Numerical Accuracy

A convergence study in space was performed using three different grids with a refinement ratio of $\sqrt{2}$ comparing the values of the C_l and C_d of the whole configuration. (The grids had about 2000, 4000, and 8000 points, with 64 points on the flap surface and 94 on the main element, 92 and 132, 136 and 188, respectively). Following Stern, et al.²⁶ it is then possible to check under which convergence condition the calculations are performed. This can be done by looking at the ratio R_k between the solution changes for medium-fine and coarse-medium solutions. In this case, a value of $R_k = 0.1546$ was found, which means a monotonic convergence condition that allows an estimate for the order of accuracy and the leading-order term of the space discretization error of the solution. For this, generalized Richardson-extrapolation is used (see Ref. 26) giving an order of accuracy of 5.4 against an expected theoretical value of 2. This result for the order of accuracy means that the solutions are not in the asymptotic range and that the leading-order term of the series expansion estimating the error underpredicts the error. The uncertainty U_{C_l} , not the error on the C_l value, thus, will be estimated.²⁶ When a correction factor accounting for the higher-order terms²⁶ is used, a value of $U_{C_l} = \pm 0.0198$ is found. When a similar analysis is performed for the C_d values, an uncertainty of $U_{C_d} = \pm 5.25 \times 10^{-5}$ is found for the drag coefficient.

Numerical Results

For the prediction of the transition point in the present analysis, an n factor equal to 7 was chosen based on previous experience with the design and wind-tunnel testing of the wing airfoil for the general aviation aircraft EXTRA 400 (Ref. 19). The grid used was the most refined used in the accuracy analysis (197×40 points).

The 3.0% gap/1.0% overlap case will be especially compared with the experimental findings. From Fig. 8 it can be noticed that

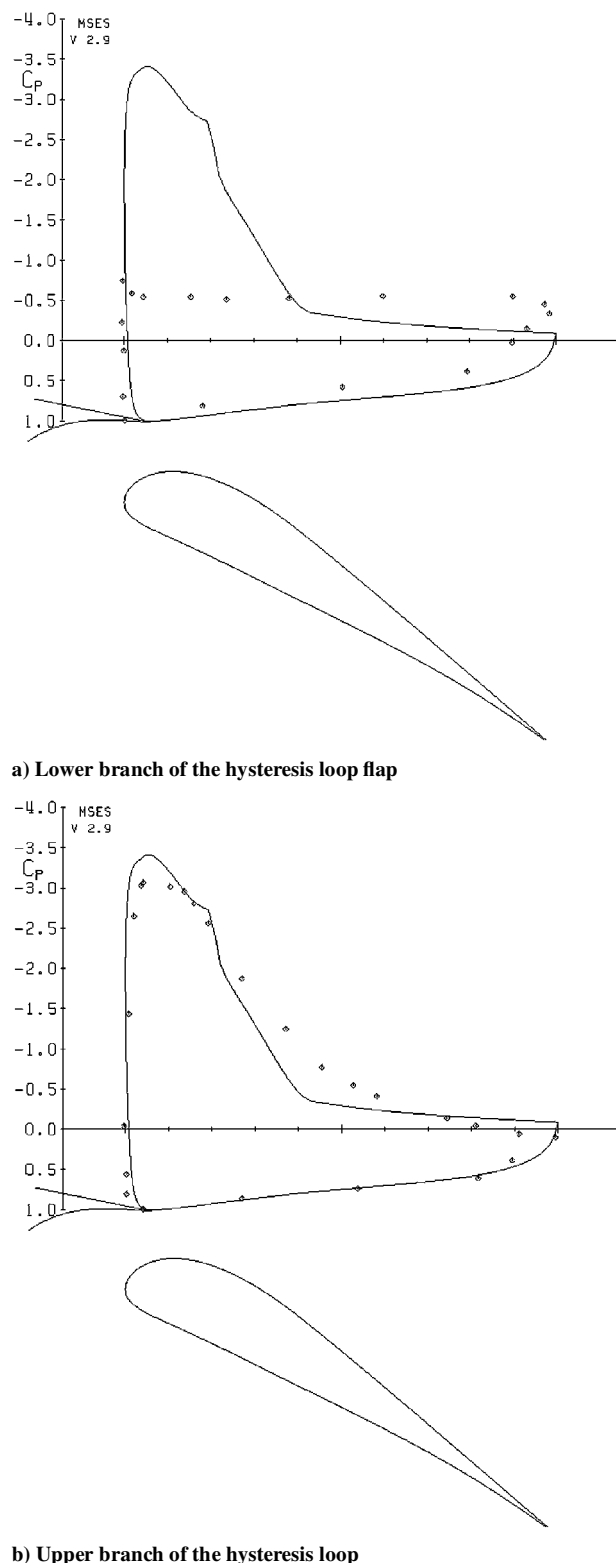


Fig. 8 Pressure distribution on the flap for $\alpha = 8$ deg, gap 3%/overlap 1%; experimental results vs computational predictions, $Re = 2 \times 10^6$, NACA 63-415 airfoil with slotted flap: —, calculated.

the pressure distribution over the flap as computed appears to be physically different from the experimental results. The computed model predicts a small laminar bubble at about 20% of the flap chord followed by a turbulent separation that approaches the reattachment point of the bubble when α is increased. This result is very different from the sudden leading-edge stall observed in the experiments. No relevant turbulent separation previous to bursting is evident from the experimental pressure plots on the flap. Figures 9 and 10 show a typical skin-friction coefficient and boundary-layer parameters (δ and θ) distribution as given by MSES in this situation. On the upper surface, the skin friction becomes zero at the location of laminar separation $x/c = 0.857$, and it stays negative over the length of the bubble before being zero again at turbulent reattachment, $x/c = 0.868$. After turbulent reattachment, it becomes zero again at about $x/c = 0.92$, being the location of the predicted turbulent separation. When Fig. 10 is examined, both θ and δ display a large increase after turbulent separation before decreasing in the wake. The stall behavior on the flap is controlled by the turbulent separation proceeding from the trailing edge, with transition taking place in the bubble just before the reattachment point. The experiments show, however, that stall suddenly takes place on the flap as a result of bursting of the laminar bubble, with no previous relevant separation taking place on the flap surface. Consequently, MSES underpredicts the lift and overpredicts the drag. To show this, the computed C_l - C_d polar and C_l - α curves for gap 3.0% overlap 1% are compared with the measured ones in Fig. 6. The large separated region after turbulent separation predicted by the code is responsible for these discrepancies. The presence of unsteady structures in the flow, which is, of course, not modeled in the code, may well be one of the reasons for this result.

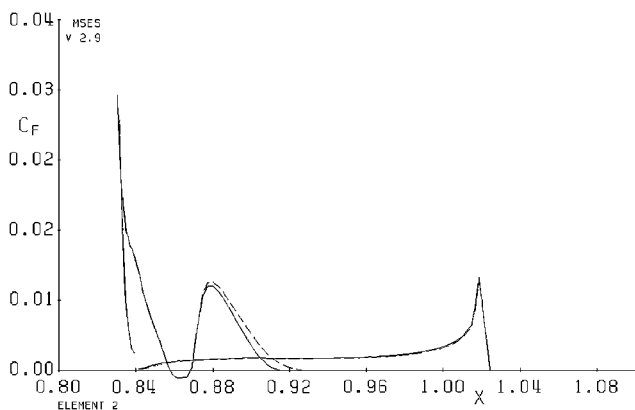


Fig. 9 Friction coefficient C_f over the flap showing laminar bubble (negative C_f) and turbulent separation, $Re = 2 \times 10^6$, NACA 63-415 airfoil with slotted flap: ---, $\alpha = 10$ and —, $\alpha = 11.5$.

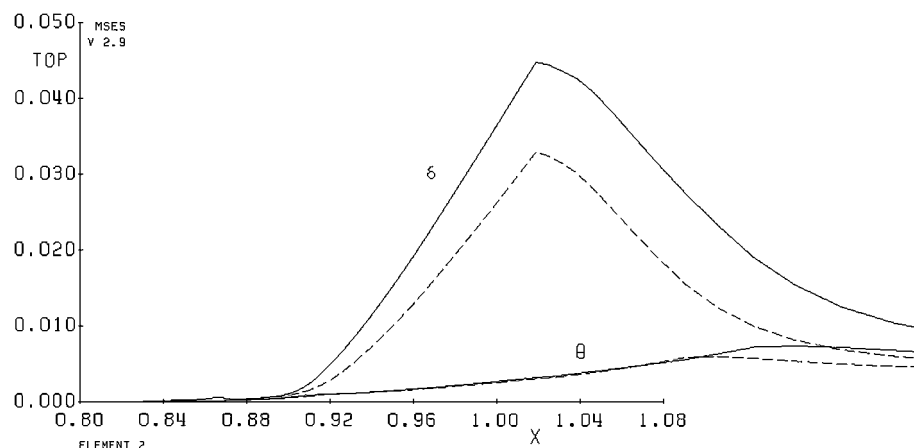


Fig. 10 Displacement δ and momentum θ thickness on the flap, $Re = 2 \times 10^6$, NACA 63-415 airfoil with slotted flap: ---, $\alpha = 10$ and —, $\alpha = 11.5$.

Bursting Prediction and Unsteadiness of Low-Reynolds-Number Laminar Separation

The flaw found in the numerical predictions of bursting onset suggests that the modeling, if not the understanding of the physics involved, is still lacking. In this section, an attempt is made to indicate what seems to be missing in the classical model of a laminar separation bubble.

The region where the flow reattaches to the surface has always been described as turbulent and steady in the mean flow. This is probably true at higher Reynolds numbers Re , where transition is more readily connected with viscous primary instabilities, that is, Tollmien-Schlichting waves amplification without necessarily a vorticity maximum away from the wall. At lower Reynolds numbers, however, available experimental evidence shows that a different behavior may be expected.

Gaster²⁷ first observed in his experiments that low-frequency oscillations seemed to be a characteristic of low Reynolds number Re bubbles. These oscillations were especially strong in long bubbles; a patch of high-frequency turbulence formed intermittently in the early stages of transition, delaying the formation of a continuous turbulent signal to a position much more downstream than in the higher Reynolds number Re , short bubbles he tested. Gleyzes et al.²⁸ experimentally analyzed the transitional flow over the surface of an ONERA LC-100-D airfoil at Reynolds numbers equal to 0.5×10^6 and higher. They focused on the long bubble obtained after bursting. Flow visualizations showed the formation of well-defined vortical structures in the rear region of this long bubble due to the appearance of an inflection point, that is, a vorticity maximum, in the separated laminar shear layer velocity profile (a so-called inviscid primary instability).

These structures were seen to characterize strongly the first stages of turbulent boundary layer development and to be quite persistent in the ensuing turbulent flow as well. In both investigations, however, no additional efforts were made to better understand what was going on, nor to identify the parameters involved. No more recent experiments on the topic are known to the authors.

More recently, Ripley and Pauley²⁹ reproduced numerically Gaster's experiments,²⁷ using an unsteady laminar Navier-Stokes solver. They identified the aforementioned structures with the occurrence of vortex shedding in the rear region of the bubble. A large-scale laminar vortex shedding resulted for the long bubble. The shedding was indeed found also for the short bubbles tested in Gaster's work. In this case, however, the frequency was higher, and the strength of the disturbance significantly lower. Time averaging the unsteady results, Ripley and Pauley found that the surface pressure distributions matched Gaster's findings and that the streamlines showed the classical steady closed bubble pattern (Fig. 1). Similar numerical findings were reported for an Eppler 387 airfoil.²⁹ The same vortex shedding occurrence was later confirmed by the numerical results obtained by Tatineni and Zhong over the APEX airfoil.³⁰

The analyses of Ripley and Pauley²⁹ and Tatineni and Zhong³⁰ were two dimensional and neglected completely any small-scale turbulence effect. Their results clearly show, however, that the laminar part of the bubble is not a region of stagnant flow but rather a region where shedding of well-defined vortical structures periodically occurs. These structures and their effect on the mean flow grow stronger when the Reynolds number Re drops. Moreover, in the Reynolds number Re range where they are present, these structures seem to grow stronger when the short bubble approaches bursting conditions and finally turns into a long one. In the short bubble far from bursting, the reattachment region could indeed be substantially steady or weakly unsteady in the mean flow, as well as, most likely, fully turbulent: The laminar structures are weaker in this case, and they are likely to dissipate rapidly after reattachment. Close to bursting and in the long bubble, the reattachment region would instead be characterized by a strong shedding of laminar structures, long persisting in the turbulent flow developing behind the bubble. This difference in the local stability characteristics of the laminar bubble may well be a signal for determining the onset of bubble bursting conditions. All bursting predictors developed so far assume a substantially steady, stagnant flow in the laminar part of the bubble. This assumption appears to be incorrect, especially at lower Reynolds numbers and may explain their poor performance in this range. This difficulty of an accurate prediction of transition onset position stems also readily from the preceding discussion: The customary assumption that transition occurs at the laminar separation point³¹ is found to be inadequate, especially for the low-Reynolds-number Re range. When the laminar boundary layer is stable enough to avoid this early breakdown, the prediction of transition onset is indeed a big challenge due to the number of parameters involved.³²

Conclusions

The problem of bubble bursting and stall hysteresis has been presented and discussed. The relevance and the danger of bursting at high lift has been pointed out, and the importance of an accurate prediction of this phenomenon has been stressed, not only for single-element airfoils at low Reynolds number Re , but also for multi-element slotted configurations, where the possibility of bursting has been only recently discovered.

The experimental and numerical results obtained on a single-slotted flap configuration designed for the wing of a general aviation aircraft were presented. The results clearly show that current numerical design codes are incapable of predicting bursting occurrence. This is indeed a major cause for concern: Once bursting occurs, it can give rise to a large hysteresis loop in the C_l - α curve. The angle of attack has to be lowered appreciably to regain prestall conditions.

A literature review was carried out showing that the current understanding of the physics underlying the bubble bursting phenomenon is still lacking of many issues, most of them related to the structure of the transitional region. A number of crucial points, especially related to the unsteadiness of the laminar separation, have been identified as currently missing for an effective bursting prediction.

Further research will focus on the importance of the laminar unsteadiness for the structure of the bubble, especially close to and after bursting conditions. Unsteady experiments and unsteady Navier-Stokes calculations will be performed to improve the existing bursting prediction methods.

References

- Shum, Y. K., and Marsden, D. J., "Separation Bubble Model for Low Reynolds Number Airfoil Applications," *Journal of Aircraft*, Vol. 31, No. 4, 1994, pp. 761-766.
- Drela, M., and Giles, M. B., "Viscous-Inviscid Analysis of Transonic and Low Reynolds Number Airfoils," *AIAA Journal*, Vol. 25, No. 10, 1987, pp. 1347-1355.
- Drela, M., "Two-Dimensional Transonic Aerodynamic Design and Analysis Using the Euler Equations," Ph.D. Dissertation, Dept. of Aeronautics and Astronautics, Massachusetts Inst. of Technology, Cambridge, MA, 1985.
- Eppler, R., *Airfoil Design and Data*, Springer-Verlag, Berlin, 1990.
- Lindblad, I. A. A., and de Cock, K. M. J., "CFD Prediction of Maximum Lift of a 2D High Lift Configuration," AIAA Paper 99-3180, June 1999.
- van den Berg, B., "Physical Aspects of Separation in Three-Dimensional

Flows," *Proceedings of the Seminar in Boundary-Layer Separation in Aircraft Aerodynamics*, Delft Univ. of Technology, Delft, The Netherlands, 1997, pp. 109-126.

⁷Wu, J. Z., Tramel, R. W., Zhu, F. L., and Yin, X. Y., "A Vorticity Dynamics Theory of Fully Three-Dimensional Flow Separation near a Generic Separation Line," AIAA paper 99-3695, 1999.

⁸Rist, U., Maucher, U., and Wagner, S., "Direct Numerical Simulation of Some Fundamental Problems Related to Transition in Laminar Separation Bubbles," *Computational Fluid Dynamics '96*, edited by J.-A. Désidéri, C. Hirsch, P. Le Tallec, M. Pandolfi, and J. Périaux, Wiley, 1996, pp. 319-325.

⁹Biber, K., "Physical Aspects of Stall-Hysteresis on an Airfoil with Slotted Flap," AIAA Paper 95-0440, Jan. 1995.

¹⁰Biber, K., and Zumwalt, G. W., "Hysteresis Effects on Wind-Tunnel Measurements of a Two-Element Airfoil," *AIAA Journal*, Vol. 31, No. 2, 1993, pp. 326-330.

¹¹Gault, D. E., "A Correlation of Low-Speed Airfoil Section Stalling Characteristics with Reynolds Number and Airfoil Geometry," NACA TN 3963, March 1957.

¹²Smith, A. M. O., "Aerodynamics of High-Lift Airfoil Systems," *Fluid Dynamics of Aircraft Stalling*, CP-102, AGARD, 1972, pp. 10-1-10-26.

¹³Chow, R. R., and Chu, K. W., "Navier-Stokes Solution for High-Lift Multi-Element Airfoil System with Flap Separation," AIAA Paper 91-1623, 1991.

¹⁴Balleur, J. C. L., and Néron, M., "Une Méthode d'Interaction Visqueux Non-Visqueux pour Ecoulements Incompressibles Hypersustentés sur Profils Multi-Corps en Régime de Décollement Profond," *High-Lift Systems Aerodynamics*, CP-515, AGARD, 1993.

¹⁵Crabtree, L. F., "Effects of Leading-Edge Separation on Thin Wings in Two-Dimensional Incompressible Flow," *Journal of the Aeronautical Sciences*, Vol. 24, No. 8, 1957, pp. 597-604.

¹⁶Horton, H. P., "A Semi-Empirical Theory for the Growth and Bursting of Laminar Separation Bubbles," Aeronautical Research Council, CP-1073, London, 1969.

¹⁷van Ingen, J. L., "On the Calculation of Laminar Separation Bubbles in Two-Dimensional Incompressible Flow," *Conference Proceedings on Flow Separation*, CP-168, AGARD, 1975, pp. 11-1-11-16.

¹⁸Dini, P., and Maughmer, M. D., "A Computationally Efficient Modeling of Laminar Separation Bubbles," *Proceedings of the Conference in Low Reynolds Number Aerodynamics*, Univ. of Notre Dame, Notre Dame, IN, June 1989.

¹⁹Tromp, E., "Design of Single Slotted Flaps for the EAGLET," M.S. Thesis, Dept. of Aerospace Engineering, Delft Univ. of Technology, Delft, The Netherlands, June 1997.

²⁰Dushin, A. B., "Aerodynamic Design and Tests of Wing Airfoils for Low-Speed Application," M.S. Thesis, Dept. of Aerospace Engineering, Delft Univ. of Technology, Delft, The Netherlands, Nov. 1998.

²¹Foster, D. N., and Lawford, J. A., "Experimental Attempts to Obtain Uniform Loading over Two-Dimensional High-Lift Wings," Royal Aircraft Establishment, Rept. RAE-TR68283, Farnborough, England, U.K., 1968.

²²Jones, B. M., "Measurement of Profile Drag by the Pitot-Traverse Method," Aeronautical Research Council, R&M No. 1688, London, 1936.

²³Allen, H. J., and Vincenti, W. G., "Wall Interference in a Two-Dimensional Flow Wind Tunnel with Consideration of the Effect of Compressibility," NACA Rept. 782, 1944.

²⁴Kline, S. J., and McClintock, F. A., "Describing Uncertainties in Single-Sample Experiments," *Mechanical Engineering*, Vol. 75, Feb. 1953, pp. 3-8.

²⁵van Ingen, J. L., "Teaching and Research in Boundary-Layer Flows," *Proceedings of the Seminar in Boundary-Layer Separation in Aircraft Aerodynamics*, Delft Univ. of Technology, Delft, The Netherlands, 1997, pp. 139-162.

²⁶Stern, F., Wilson, R. V., Coleman, H. W., and Paterson, E. G., "Comprehensive Approach to Verification and Validation of CFD Simulations—Part 1: Methodology and Procedures," *Journal of Fluids Engineering*, Vol. 123, Dec. 2001, pp. 793-810.

²⁷Gaster, M., "The Structure and Behaviour of Laminar Separation Bubbles," CP-4, AGARD, May 1966.

²⁸Gleyzes, C., Cousteix, J., and Bonnet, J. L., "Bulbe de Décollement Laminaire avec Transition (Théorie et Expérience)," *L' Aéronautique et L' Astronautique*, No. 80, 1980, pp. 41-57.

²⁹Ripley, M. D., and Pauley, L. L., "The Unsteady Structure of Two Dimensional Steady Laminar Separation," *Physics of Fluids A*, Vol. 5, No. 12, 1993, pp. 3099-3106.

³⁰Tatineni, M., and Zhong, X., "A Numerical Study of Low Reynolds Number Separation Bubbles," AIAA Paper 99-0523, Jan. 1999.

³¹Masad, J. A., and Malik, M. R., "On the Link Between Flow Separation and Transition Onset," AIAA Paper 94-2370, June 1994.

³²Reshotko, E., "Stability and Transition of Boundary Layers," *Progress in Astronautics and Aeronautics*, Vol. 112, 1988, pp. 278-311.

A. Plotkin
Associate Editor